2018-05

Environmental sustainability of light-driven processes for wastewater treatment applications

Foteinis, S

10.1016/j.jclepro.2018.02.038
Journal of Cleaner Production
Elsevier BV

Environmental sustainability of light-driven processes for wastewater treatment applications

Spyros Foteinis[a], Alistair G. L. Borthwick[b], Zacharias Frontistis[c], Dionissios Mantzavinos[c], Efthalia Chatzisymeon[b*]

[a] Senior Engineer, Greek Public Power Corporation (PPC) Renewables S.A., Kapodistriou 3, Ag. Paraskeui, GR-15343, Attica, Greece

[b] School of Engineering, Institute for Infrastructure and Environment, University of Edinburgh, Edinburgh EH9 3JL, United Kingdom

[c] Department of Chemical Engineering, University of Patras, Caratheodory 1, University Campus, GR-26504 Patras, Greece

* Corresponding author: e.chatzisymeon@ed.ac.uk, tel.: +44(0)1316505711

Abstract

A comparative analysis is presented of light-driven advanced oxidation processes in terms of environmental sustainability. Photochemical oxidation has proven a viable option for treating emerging and priority pollutants at laboratory scale. Nevertheless, as a nascent technology, photocatalysis is yet to be widely applied at large-scale water treatment plants. This paper presents a powerful tool that should enable stakeholders to develop sustainable, large-scale, photocatalytic treatment plants by providing knowledge of environmental sustainability and hotspots (where technological flaws

have high environmental impact) and understanding as to how process sustainability can be improved through scenario analyses. The following processes were examined: natural and simulated solar photolysis, solar photo-Fenton without hydrogen peroxide addition (solar/Fe), solar photo-Fenton (solar/Fe/H_2O_2), photolysis under UV-A irradiation (UV-A), titania-mediated photocatalysis (UV-A/TiO_2), photolysis under UV-C irradiation (UV-C), and UV-C treatment with hydrogen peroxide addition (UV-C/H_2O_2). Actual life cycle inventory data were collected at bench scale, and the environmental performances estimated by means of life cycle assessment. Effective removal of 1μg of 17α-ethynylestradiol per liter of wastewater, a commonly occurring micropollutant and endocrine disrupting chemical, was used as the functional unit. Solar photolysis exhibited an environmental footprint about 23 times higher than solar/Fe. Solar/Fe/H_2O_2 minimized the environmental footprint. Being energy intensive, simulated solar irradiation had a much higher (~ 5-fold) environmental footprint than natural solar light. UV photolysis exhibited low environmental impact, with UV-C found to be about 3 times more environmentally friendly than UV-A photolysis. Addition of TiO_2 to UV-A and H_2O_2 to UV-C caused their total environmental impacts to decrease by about 97% and 88%, implying that UV-A/TiO_2 was better than UV-C/H_2O_2. In terms of total environmental footprint, the AOPs descend in the following order: solar photolysis > UV-A > UV-C > solar/Fe > UV-A/TiO_2 > UV-C/H_2O_2 > solar/Fe/H_2O_2. The environmental sustainability of all processes was directly proportional to treatment efficiency but inversely proportional to treatment time (due to the large energy input per unit time). Although reagent use (i.e. titania, iron, and hydrogen peroxide) was not associated with high environmental impact, its addition greatly improved process efficiency as well as environmental sustainability. For all examined light-driven processes, the main environmental

hotspot was electricity consumption. Introduction of renewable energy sources could reduce the environmental footprint of oxidation processes by up to 87.5%.

Keywords: water purification; estrogens; photocatalysis; LCA; EDCs; EE2

1. Introduction

Trace- or micro-pollutants are synthetic chemicals of emerging environmental and health concern that have recently been detected in the aquatic environment (Tiedeken, 2017). Several hundred EDCs have been measured in humans and wildlife, even in such remote places as the Arctic (Birnbaum, 2013). There is growing evidence that these pollutants have adverse effects on human health and living organisms. Trace-pollutants can act, or have the potential to act, as endocrine-disrupting chemicals (EDCs) that cumulatively interfere with the endocrine system of living organisms and cause genetic abnormalities, infertility, feminization, increased cancer rates, trigger Alzheimer disease, etc. (Rochester, 2013). EDCs derive from the chemical processing industry in the form of drugs, surfactants, cosmetics, and other personal care products, which usually end up in the sewage system. Synthetic estrogens are EDCs that are found in increasing concentrations in natural waters (Zhang et al., 2014) and wastewater (Mohagheghian et al., 2014). A representative synthetic estrogen is 17α-ethynylestradiol (EE2), which is the basic component of the contraceptive pill. EE2 is more stable in an aqueous environment and has greater estrogenic potency (~11–27

71 times) than natural estrone (E1) and estradiol (E2). Continuous exposure to EE2, even
72 to concentrations of μg/L, has been found to cause bodyweight loss, accelerate
73 vaginal opening, alter estrous cycles in young animals, and damage fish populations
74 (Frontistis et al., 2015).

75 Due to their xenobiotic and non-biodegradable nature, conventional biological
76 wastewater treatment plants (WWTPs) cannot effectively remove EDCs, which in
77 turn are discharged into receiving waters. To overcome this, it is necessary to add
78 robust tertiary treatment technologies to existing WWTPs. Of the technologies
79 available for the removal of EDCs, light-driven advanced oxidation processes (AOPs)
80 offer considerable promise. The effectiveness of AOPs is mainly due to the formation
81 of reactive oxygen species (ROS), such as hydroxyl radicals ($HO^{\bullet}$), which
82 subsequently oxidize the organic content of water samples. AOPs include solar, UV-
83 A and UV-C photolysis and photocatalysis, usually accelerated by adding titania
84 (TiO_2) (i.e. heterogeneous catalysis) (Lee et al., 2017), hydrogen peroxide (H_2O_2)
85 and/or iron (Fe^{2+}) to form the photo-Fenton reagent (i.e. homogeneous catalysis)
86 (Clarizia et al., 2017). To date, several studies have investigated the treatment of EE2-
87 contaminated water by means of UV photocatalysis (Madsen and Søgaard, 2012), UV
88 photolysis (Marinho et al., 2013; Sichel et al., 2011), and solar photocatalysis (Kim et
89 al., 2017; Koutantou et al., 2013). Even so, apart from UV-C photolysis, other light-
90 driven AOPs are still nascent technologies, not yet applied at industrial-scale.

91 AOPs are energy intensive, with high operating cost and elevated
92 environmental footprint (Chatzisymeon et al., 2013). Solar photo-Fenton AOPs have
93 high chemical demand, and generate residual fluxes with negative environmental
94 impacts, such as sludge contaminated by metal ions, exhausted solid catalysts, etc.
95 (Rodríguez et al., 2016). Previous research has focused on the degradation efficiency

and techno-economic feasibility of AOPs, without detailed consideration of environmental sustainability (Rodríguez et al., 2016). A brief review of existing studies on AOPs environmental sustainability is given by (Ioannou-Ttofa et al., 2016).

In order for AOP technology to reach prototype-scale applications, it must be acceptable from an environmental perspective. To achieve this, the environmental sustainability of each AOP should first be assessed at bench- or pilot-scale, in order to identify merits and drawbacks, establish the main environmental impact hotspots, and assess ways of reducing the total environmental footprint through scenario and sensitivity analyses. By determining the optimal environmental performance of AOPs, the technology could be effectively scaled up to sustainable, large-scale applications in water treatment works.

This paper describes a comparative life cycle assessment (LCA) of seven well-established light-driven AOPs, namely: solar, solar/Fe, solar/Fe/H_2O_2, UVA, UVA/TiO_2, UVC, and UVC/H_2O_2. The aim is to identify the strengths and weaknesses of AOPs from an environmental sustainability perspective, thus enabling process scale up. LCA methodology is employed, in accordance with ISO 14040 and ISO 14044 (ISO, 2006a, b), using SimaPro 8. The assessment was made using life cycle inventory (LCI) data collected from bench-scale experiments, rather than extracted from a database. The results should provide researchers, decision- and policy-makers, and the water treatment industry with a better understanding of the environmental sustainability of light-driven AOPs, which in turn should help advance the technology so that it becomes ready for industrial-scale application. To the best of the authors' knowledge this is the first study to date dealing with LCA of several light-driven oxidation processes. Many publications focus on comparing several irradiation sources in terms of ability to decontaminate/disinfect water and

wastewater. Assessment of environmental sustainability of such processes, including both solar and UV-irradiated techniques, is presently missing from the literature.

Of the various methodologies used to assess the environmental sustainability of a product or process, the most commonly utilized are multi-criteria analysis (MCA), environmental performance indicators (EPIs), and life cycle assessment (LCA) (Hermann et al., 2007). MCA compares and ranks alternative options, and evaluates environmental consequences according to established criteria. However, its weakness lies in the subjectivity of the weighting step, necessary to evaluate different criteria. EPIs estimate the current or past environmental performance of an organisation and compare it against a set of targets; however, the usefulness of EPIs is limited by insufficient data availability (Hermann et al., 2007). LCA offers an effective means of including environmental considerations in the design, production, use, and disposal of a product (Foteinis et al., 2011). LCA is a tool for the systematic evaluation of environmental impacts, which provides insight into the overall performance and relative contributions of different stages within the product lifespan (Hermann et al., 2007).

2. Materials and methods

Data used in the comparative LCA analysis were obtained from laboratory experiments, described by Frontistis et al. (2011, 2012, 2015). All experiments were carried out under the same ambient temperature and water conditions. Table 1 lists the optimum operating conditions assayed for each light-driven process. In all cases, the wastewater sample was stirred by a 50 W magnetic stirrer and the ambient temperature kept constant at 25±2 ºC. Energy required to keep the temperature

constant was external to system boundaries, while the stirrer was assumed to operate at 30 W (i.e. not at full power). At industry scale, wastewater pumping would replace the magnetic stirrer. Simulated solar irradiation was emitted by a Newport, model 96000, 150 W solar simulator system. The UV-A and UV-C experiments were conducted in an immersion well, batch type, laboratory-scale photoreactor (Ace Glass, Vineland, NJ, USA). UV-A irradiation was provided by a 9 W lamp (Radium Ralutec, 9W/78, 350–400 nm). UV-C irradiation was provided by an 11 W low-pressure mercury lamp (Phillips, TUV PL-S). The Fe^{2+} ionic solution used in the experiments was in the form of $FeSO_4 \cdot 7H_2O$ (≥ 99%, Sigma-Aldrich). H_2SO_4 was added in order to regulate the initial water pH. TiO_2 P25 was donated by Evonik Industries, and H_2O_2 (35% w/w) was purchased from Merck.

3. Environmental sustainability analysis

To assess the environmental sustainability of light-driven AOPs, LCA methodology was employed, as detailed in ISO 14040 and 14044 (ISO, 2006a, b). Bench-scale experimental results were utilized by the environmental model. The timespan covered 2010 to the present date, the geographical boundaries encompassed Greece and similar countries, and average technology was assumed. For the foreground system, primary inventory data were collected for laboratory-scale experiments, while, for the background system, data were used regarding the most recent average technology (e.g. for electricity the average technology mix in Greece was imported from the ecoinvent database).

3.1 Functional unit

169 The functional unit selected to quantify the performance of a light-driven AOP was
170 the effective removal of 1 μg EE2 per liter of treated wastewater. The life cycle
171 inventory (LCI) for each AOP under study was then normalized per functional unit
172 (ISO, 2006a, b) in order to study the environmental performance of the different
173 technologies. Attributional life cycle assessment (ALCA) was used because it
174 estimates the environmental impacts of a product or system according to the delivery
175 of a specified quantity of the functional unit (Chatzisymeon et al., 2016).

176 **3.2 System boundaries and life cycle inventory (LCI)**

177 The system boundaries define which unit processes (the smallest elements for which
178 input and output data are quantified in the LCI) are included within the LCA (ISO,
179 2006a). Energy and raw material requirements, waterborne emissions, and the
180 materials' disposal or recycling are included within system boundaries.

181 For the solar and UV photoreactor AOPs, LCI data could not be identified and
182 so their primary materials, i.e. glass, lamps, and the stirrer, were taken into account. It
183 was assumed that both photoreactors have similar dimensions and materials, and that
184 all experiments were carried out at the same ambient temperature. Two different
185 scenarios were examined for the solar AOPs. The first scenario comprised the
186 photoreactor and lamp (i.e. simulated solar irradiation), whereas the second scenario
187 did not include the lamp (i.e. natural solar irradiation). The latter scenario is closer to
188 actual operating conditions of solar AOPs. Following Ioannou-Ttofa et al. (2017), the
189 photoreactor glass was assigned a useful lifespan of five years (10 h/d operation, all
190 year round). Recycling was also incorporated. Photoreactor lamps are not included in
191 SimaPro's proprietary life cycle inventory (LCI) databases, and so the LCI data were
192 obtained from relevant literature (Garrett and Collins, 2009; OSRAM, 2016). The

193 data were re-scaled according to the power requirements of each process and input to
194 SimaPro in order to simulate the environmental impact of each lamp under study.
195 Data on the stirrer used to mix effluent were not available in SimaPro's proprietary
196 LCI databases, and so were substituted by relevant data concerning the LCI of a low-
197 power motor (AAB, 2002), re-scaled to fit the rated output of the stirrer under study,
198 and used as input to SimaPro.

199 Information on the Fe^{2+} ion as iron sulphate was supplied from the SimaPro
200 LCI databases. Residual Fe^{2+} in the treated wastewater was also taken into account as
201 waterborne emission. Data on H_2O_2 and H_2SO_4 reagents were obtained from
202 proprietary LCI databases. Energy used to drive each process was supplied as
203 electricity from the Greek energy grid, which is fossil fuel-dependent and comprises
204 54% lignite, 11% crude oil, 17% natural gas, and 18% renewable energy (Ioannou-
205 Ttofa et al., 2016). To carry out the comparative analysis, from an environmental
206 perspective, of light-driven AOPs, the final use and disposal route of treated effluent
207 was taken to be external to system boundaries. In other words, cradle-to-gate (treated
208 effluent) was used.

209

210 Table 1.

211

212 **3.3 Life cycle impact assessment (LCIA)**

213 Life cycle impact assessment (LCIA) relates the data inventory to specific
214 environmental impacts and damages (ISO, 2006a, b). ReCiPe was chosen for the
215 LCIA as a robust method that comprises both midpoint and endpoint impact/damage
216 approaches which examine different stages in the cause-effect chain to calculate

impact (Chatzisymeon et al., 2016). The endpoint, or damage-oriented, approach translates environmental impacts into issues of concern, such as human health, natural environment, and natural resources. Endpoint results are associated with higher levels of statistical uncertainty, compared to midpoint, due to data gaps and assumptions stacking up along the cause-effect chain, but are easier for decision- and policy-makers to comprehend (Chatzisymeon et al., 2016). Given that this is a comparative LCA, results are compared using the following three endpoint damage categories: "Human Health", "Resources", and "Ecosystems". These can be also aggregated into a single score, which makes interpretation simpler.

A hierarchist perspective (H), based on the most common policy principles, was invoked within ReCiPe along with European normalization and average weighting. Decisions whether or not to include information in the H model are based on mean scientific consensus, and it assumes that, with proper management, environmental impacts can be avoided (Chatzisymeon et al., 2016), thus fitting better the goal and scope of the comparative analysis.

Moreover, in order to ensure accuracy and transparency of the LCA, the primary LCI data along with data used for the background system were verified against information from the open literature (Chatzisymeon et al., 2013; Gimenez et al 2015). Light-driven AOPs comprise a nascent technology for wastewater treatment, and so comparative environmental studies based on similar operating conditions and similar initial organic loads are needed; however, information on these important parameters is scarce.

3.4 Energy consumption

The energy consumption of artificial lighting constitutes a major fraction of the operating costs in UV treatment. Bolton et al. (2001) introduced the electric energy per order, E_{EO}, defined as the energy required for 90% degradation of a pollutant per m^3 of contaminated water. E_{EO} (kWh/m^3/order), for a batch-operated reactor, is calculated from the following equation:

$$E_{EO} = \frac{P \times t \times 1000}{V \times 60 \times \log(C_i/C_f)} \quad (1)$$

where P is the electrical power of the irradiation source (kW), t is the irradiation time (min), V is the volume of the treated effluent (L), and C_i and C_f are the initial and the final pollutant concentrations (mg/L), respectively.

4 Results and discussion

To render the analysis both comprehensive and straightforward to follow, the results for the solar and UV irradiation light sources are considered separately. Then, a comparative analysis of all processes follows in order to identify the most promising result in terms of environmental sustainability. Finally, a sensitivity analysis is carried out using scenarios to investigate the effect of the main environmental hotspots and to propose "greener" alternatives by which to improve sustainability.

4.1 Environmental sustainability of solar-driven AOPs and effects of Fe^{2+} and H_2O_2

Results provided by ReCiPe for natural and simulated solar-driven photolysis/photocatalysis at endpoint level (Figure 1) show that simulated (artificial light) and natural solar photolysis yielded by far the highest environmental footprints of ~11 mPt and ~2 mPt per functional unit, respectively. The environmental footprint

264 due to photolysis was ~ 23 times larger than that of simulated/natural solar/Fe, using
265 low reagent concentration (5 mg/L Fe^{2+}), with scores of 0.477 mPt (artificial light)
266 and 0.089 mPt (natural light). For photolysis, as well as all other AOPs, the main
267 environmental hotspot was electricity use derived from Greece's fossil fuel-dependent
268 electricity mix. At the time of writing, electricity systems worldwide use fossil fuels
269 for bulk power generation (Berill et al., 2016) and so the foregoing results are
270 presently valid for Greece, Europe and beyond. Indirect impacts of the use of
271 electricity from fossil fuels can be traced mainly to the "Human Health" damage
272 category, followed by "Resources", and less so the "Ecosystem" (Chatzisymeon et al.,
273 2016). "Human Health" damage is affected by fossil-fuel mining and combustion,
274 which release toxic materials including metals, sulphur, and polycyclic aromatic
275 hydrocarbons (PAHs) to the environment (Chatzisymeon et al., 2016). Fossil-fuel
276 extraction and burning contribute to climate change. Natural gas extraction also
277 releases SO_2. Impacts from coal arise from tailpipe emissions after combustion and
278 emissions during blasting at coal mines (Berill et al., 2016). "Resources" damage is
279 primarily caused by depletion of fossil fuels for electricity generation and of mineral
280 resources used to construct equipment required for resource extraction, processing
281 and consumption, and to a lesser degree by equipment related to AOPs (i.e. the stirrer
282 and photoreactor). Turning to "Ecosystem" damage, phosphate leachate from coal
283 mining spoil landfill sites and the emission of nitrogen oxides from combustion of
284 fossil-fuel directly impact on acidification and eutrophication. Waterborne metal
285 emissions from coal power plants, natural gas extraction (particularly of bromine) and
286 from disposed coal mine spoil (nickel and magnesium) affect ecotoxicity (Berill et al.,
287 2016; Ioannou-Ttofa et al., 2016).

288 Use of simulated irradiation raised the environmental impact because the total
289 environmental footprint of simulated solar photolysis and photocatalysis is about a
290 factor of 5 higher than natural solar light. This is attributed to electricity consumption
291 by the lamp (~ 81.3% of total environmental footprint), and to a much lower degree to
292 the lamp material (~ 0.05% of total environmental footprint). In terms of material, the
293 stirrer (i.e. motor) contributed 12.4% and 2.3% to the total environmental footprints
294 for natural and simulated solar photolysis. Finally, the photoreactor material (glass)
295 made a very low contribution to the total environmental footprint, 0.257% and
296 0.0494% for natural and simulated solar photolysis, respectively, mainly because of
297 the long lifespan of glass whose recycling was included in the system boundaries.
298 The relatively high environmental footprint of solar photolysis is due to its low
299 treatment efficiency as it consumes energy during the stirring process while EE2 is
300 removed from wastewater.

301

302 Figure 1.

303

304 To study the environmental impacts of the more environmentally friendly
305 natural solar-driven AOPs, a separate comparison was undertaken, neglecting
306 photolysis and simulated solar irridiation. Figure 2 shows that the amount of oxidation
307 reagents used strongly affected the environmental sustainability of solar-driven AOPs,
308 with high reagent concentration improving the overall environmental sustainability of
309 solar AOPs. At low concentration of iron ions (5 mg/L Fe^{2+}) the total evironmental
310 footprint of natural solar/Fe was estimated to be 0.089 mPt, whereas when the
311 concentration was increased to 15 mg/L the total environmental footprint reduced by

about half to 0.047 mPt per functional unit (Figure 2). When H_2O_2 was also added as a reagent, the environmental sustainability of the process was further enhanced. More specifically, when keeping the iron ion concentration constant at 5 mg/L and adding 10 mg/L H_2O_2 the total environmental footprint of the process was ~0.01 mPt per functional unit, and by increasing the H_2O_2 concentration to 17.2 mg/L the environmental footprint of the process achieved a minumum of ~ 0.356×10^{-3} mPt per functional unit.

This large reduction is attributed to: (a) increased degradation efficiency at higher H_2O_2 concentration (Table 1); (b) lower treatment time (15 min for 10 mg/L H_2O_2, and 1 min for 17.2 mg/L H_2O_2) and hence reduced energy consumption; and (c) use of low amounts of H_2O_2, a non-toxic chemical without elevated environmental impact. As mentioned before, the environmental impacts of solar/Fe can be traced back to Greece's fossil fuel-dependent electricity mix used to drive the stirrer. The contributions of electricity consumption to the total environmental footprint of natural solar/Fe (5 mg/L and 15 mg/L), natural solar/Fe/H_2O_2 (10 mg/L) and natural solar/Fe/H_2O_2 (17.2 mg/L) were 87.4%, 87.3% and 86.5%. The photoreactor and the stirrer-drive motor made material contributions of 0.256 ± 0.02 % and 12.35 ± 0.05 %. As a non-hazardous reagent when in small concentrations, Fe^{2+} had a negligible effect in all cases (its biggest score was 0.058% in natural solar/Fe/H_2O_2 (17.2 mg/L)). Similarly, the addition of miniscule amounts of H_2SO_4 in concentrations of about 50 μL/L led to it also making a negligible contribution. For natural solar/Fe/H_2O_2, addition of hydrogen peroxide at concentrations of 10 mg/L and 17.2 mg/L contributed ~0.037% and 0.943% to total environmental footprint. The latter, higher percentage contribution is related to the overall low environmental footprint of the process (0.356×10^{-3} mPt) and the higher quantity of hydrogen peroxide used (and

337 the knock-on increased energy and materials required for its synthesis). It should be
338 noted that no H_2O_2 emissions (e.g. airborne, waterborne) or harmful by-products were
339 assumed to be generated during treatment.

340

341 Figure 2.

342

343 **4.2 Environmental sustainability of UV-A and UV-C photocatalysis**

344 Figure 3 presents the environmental footprints of UV-A and UV-C
345 photolysis/photocatalysis in terms of "Human Health", "Resources" and
346 "Ecosystems" endpoint damage categories. UV-A photolysis yields a higher
347 environmental footprint (0.309 mPt), whereas that of UV-C is about a factor of three
348 smaller (0.117 mPt). This is expected because UV-C treatment has a much higher
349 treatment efficiency due to the higher energy (Frontistis et al., 2015), compared to
350 UV-A treatment. In both cases the lamp materials hardly contributed to the total
351 environmental footprint, whereas the UV-C lamp required about 20% higher power
352 but also had significantly higher treatment efficiency (see Table 1). As a result, UV-C
353 removed 1 µg/L of EE2 at a much faster rate than UV-A treatment, requiring less
354 energy and contributing less environmental footprint per functional unit.

355 When reagents were added, the environmental footprint of both UV-A and
356 UV-C treatment was substantially reduced. Figure 3 shows that addition of titania (10
357 mg/L TiO_2) drastically reduced the total environmental footprint of UV-A treatment,
358 from ~309 µPt for UV-A photolysis to ~9.2 µPt for UV-A/TiO_2 heterogenous
359 photocatalysis. As far as UV-C treatment is concerned, the addition of H_2O_2 (10
360 mg/L) also had a profound effect, with the environmental footprint of UV-C

361 photolysis reducing from ~117 μPt for UV-C to ~13.8 μPt for UV-C/H_2O_2. These
362 large reductions (~97% for UV-A/TiO_2 and ~88% for UV-C/H_2O_2) are due to a
363 combination of improved treatment efficiency and reduced treatment time (Table 1).

364 As with solar-driven AOPs, the environmental sustainability of UV-driven
365 AOPs is enhanced by addition of small amounts of the non-hazardous reagents, TiO_2
366 and H_2O_2, leading to significant improvement in degradation efficiency and reduction
367 in treatment time, especially for UV-A treatment.

368 Electricity consumption makes the largest contribution to most damage
369 categories, reflected by its contribution to the total environmental footpint of UV-
370 driven AOPs of 88.3 ± 0.1 %. This score is dominated by electricity consumption by
371 the stirrer motor and, to a lesser degree, to the lamp(s). The stirrer motor as a material
372 was the next most important environmental hotspot with scores ranging from 9.15%
373 to 9.63% of the total environmental footpint. The lamp as a material contributed from
374 1.79% for UV-A to 2.35% for UV-C. The photoreactor as a material (glass)
375 contributed from 0.19% for UV-C to 0.29% for UV-A. The reagents TiO_2 and H_2O_2
376 contributed very low percentages, 0.236% for UV-A/TiO_2 and 0.0273% for UV-
377 C/H_2O_2, of the total environmental footprint. Even though TiO_2 had a higher impact
378 than H_2O_2, UV-C/H_2O_2 exhibited a slightly higher total environmental footprint than
379 UV-A/TiO_2, mainly due to the reduced treatment time of the latter (Table 1).

380

381 Figure 3.

382

383 **4.3 Environmental sustainability of solar versus UV-A and UV-C photocatalysis**

384 Given that photolysis invariably exhibited the highest overall environmental footprint,
385 the most promising photocatalytic processes were determined in terms of
386 environmental sustainability. Figure 4 presents a comparative analysis, using ReCiPe
387 impact assessment method, of natural solar/Fe, natural solar/Fe/H_2O_2, UV-A/TiO_2 and
388 UV-C/H_2O_2 photocatalysis. Natural solar/Fe/H_2O_2, at high reagent concentrations
389 (Fe^{2+} = 5 mg/L and H_2O_2 = 17.2 mg/L) yielded the lowest score (0.356 µPt per
390 functional unit) amongst all processes. For simulated solar irradiation, the total
391 environmental footprint of solar/Fe/H_2O_2 rose to 1.869 µPt, but nevertheless remains
392 substantially lower than all the other light-driven AOPs considered. Again, the
393 presence of iron and hydrogen peroxide oxidants, the reduced treatment time and
394 enhanced EE2 removal efficiency caused the energy demand per functional unit to be
395 minimized, lowering the environmental footprint. The next most environmentally
396 friendly AOPs were UV-A/TiO_2 (~9.2 µPt or ~96% higher than natural
397 solar/Fe/H_2O_2) and UV-C/H_2O_2 (~13.8 µPt). Both exhibited relatively high treatment
398 efficiency, with UV-A/TiO_2 requiring less treatment time to achieve EE2 removal
399 (Table 1), which meant less energy input and a lower environmental footprint than
400 UV-C/H_2O_2. Also, the lamp required higher energy to drive the UV-C/H_2O_2 process
401 (11W) than UV-A/TiO_2 (9 W). The lamps, photoreactor, and stirrer made low
402 contributions as materials to the total environmental footprints of the UV-C/H_2O_2 and
403 UV-A/TiO_2 processes. The contribution by the reagents, TiO_2 and H_2O_2, was
404 miniscule compared to electricity consumption. Finally, natural solar/Fe exhibited a
405 high overall environmental footprint, especially at low reagent concentration (5 mg/L
406 Fe^{2+}) where the value was 0.089 mPt. For a high iron concentration (i.e. 15 mg/L), the
407 total environmental footprint was halved, to 0.047 mPt per functional unit (Figures 2
408 and 4).

409 In short, all the light-driven AOPs considered in this work were limited by the
410 same environmental hotspot, namely electricity consumption from Greece's fossil
411 fuel-dependent energy mix, which dominated the contributions to ReCiPe's damage
412 categories "Human Health" and "Resources". Similar findings were obtained by
413 (Chatzisymeon et al., 2013) who compared the environmental sustainability of UV-
414 A/TiO_2 with electrochemical and wet air oxidation processes for treatment of agro-
415 industrial wastewater.

416

417 Figure 4.

418

419 The present comparison is based on bench-scale experimental data. It is expected that
420 further benefits can be achieved for all AOPs examined, in terms of lowering the
421 environmental footprint per functional unit when the processes are scaled up. For
422 example, in prototype applications, the stirring processes, which required large energy
423 inputs at bench scale, will be replaced by pumping which is more energy efficient.
424 Given that it also consumes electricity, pumping is likely to be a prime environmental
425 hotspot (as also suggested by Foteinis et al. (2018) in a study of pilot-scale Fenton
426 processes for pharmaceutical wastewater treatment).

427 Energy consumption to degrade 90% of EE2 was also estimated in order to undertake
428 a more comprehensive comparative analysis of artificial light-driven oxidation
429 processes. The corresponding treatment time was estimated either using experimental
430 values from photocatalytic tests carried out by Frontistis et al. (2015), Frontistis et al.
431 (2012) and Frontistis et al. (2011) or by extrapolating the experimental values to
432 achieve 90% removal of EE2. The results are shown in Table 2, where it is observed

433 that UVA/TiO_2 process has the lowest energy demands followed by UVC/H_2O_2,
434 solar/Fe(5mg/L)/H_2O_2, UVC, UVA, solar/Fe(15mg/L), solar/Fe(5mg/L) and
435 simulated solar process. In principle, these results are consistent with those obtained
436 from LCA (Figure 4) confirming the high dependence of AOPs on electricity
437 consumption.

438

439 Table 2.

440

441 **4.5 Sensitivity analysis**

442 The main environmental barrier to light-driven AOPs under study is electricity
443 consumption from the Greek energy mix dominated by fossil fuels. Power systems
444 based largely on renewable energy sources (RES) perform much better regarding
445 climate change and other impact categories than systems based on fossil fuels (Berrill
446 et al., 2016). A sensitivity analysis was carried out involving three energy mix
447 scenarios solely based on RES, i.e. solar, wind, and hydropower, all naturally
448 abundant in Greece, Europe and beyond. Energy storage, curtailment, and grid
449 extension were neglected because the aim of scenario analysis is purely to illustrate
450 possible pathways and futures, rather than make forecasts or predictions (Kouloumpis
451 et al., 2015). Moreover, the extra impacts caused by energy storage and grid extension
452 are likely to be of such relatively small magnitude that the environmental benefits of
453 switching to renewables would not be undermined (Berrill et al., 2016). The use of
454 RES to meet the electricity needs of light-driven AOPs is expected to lead to
455 substantial improvement in their environmental sustainability. For example, use of an
456 electricity mix solely based on photovoltaic (PV) systems (i.e. 3 kWp single-Si panels

mounted on slanted roofs) decreases the total environmental footprint of solar AOPs by about 85% and UV-driven AOPs by 87%. On the other hand, use of an electricity mix solely based on wind energy (onshore wind turbines, capacity in the range from 1 to 3 MW) further improves the environmental sustainability of light-driven AOPs because energy from wind turbines usually has a lower environmental impact than solar PVs (Chatzisymeon et al., 2016). In this case, the total environmental footprint of solar AOPs and UV-driven AOPs is decreased by about 81% compared to the initial scenario. Finally, use of an electricity mix solely based on hydropower leads to the largest decrease in total environmental footprint of light-driven AOPs by 86% (solar) and 87% (UV) because hydropower is the most environmentally friendly RES option (Ioannou-Ttofa et al., 2016).

In all cases, the highest reduction in environmental footprint occurred for the most energy intensive AOPs (i.e. simulated solar, UV-A, and UV-C, ordered from higher to lower reduction), whereas the smallest reduction occurred for the most energy efficient AOPs (i.e. solar/Fe/H_2O_2, solar/Fe, UV-A/TiO_2, and UV-C/H_2O_2, ordered from lower to higher reduction). The order of light-driven processes in terms of environmental sustainability remained the same for all scenarios; from higher to lower score: natural or simulated solar > UV-A > UV-C > natural or simulated solar/Fe > UV-A/TiO_2 > UV-C/H_2O_2 > natural or simulated solar/Fe/H_2O_2. Even so, it should be noted that UV-A/TiO_2 and UV-C/H_2O_2 exhibited similar environmental footprints when using RES.

5. Conclusions

480 This paper has investigated the environmental performance of light-driven AOPs at
481 removing an endocrine disruptor, EE2, from wastewater using actual life cycle
482 inventory (LCI) data. It was found that the environmental sustainability of light-
483 driven AOPs was directly proportional to treatment efficiency (which was expected
484 given that the chosen functional unit was the removal of 1 μg EE2 per liter of
485 wastewater), and was also inversely proportional to treatment time. Moreover,
486 electricity consumption from the fossil fuel-dependent Greek energy mix was the
487 main environmental hotspot for all examined AOPs. The Fe^{2+}, H_2O_2, and H_2SO_4
488 reagents used in light-driven AOPs were associated with low environmental impacts
489 because the chemicals did not detrimentally affect health or the eco-system, no
490 harmful by-products were generated, and only low dosages were used. Use of RES to
491 meet the electricity needs of light-driven AOPs substantially improved their
492 environmental sustainability, by up to 87% for solar- and 88% for UV-driven AOPs.

493 References
494
495 AAB, 2002. Environmental Product Declaration For Electric Motor Type 90S 4 Pole
496 (3GAA092001-ASC). ABB Motors A/S, Petersmindevej 1, DK-5000 Odense C.
497 Birnbaum, L.S., 2013. State of the Science of Endocrine Disruptors. Environmental Health
498 Perspectives 121, a107-a107.
499 Chatzisymeon, E., Foteinis, S., Borthwick, A.G.L., 2016. Life cycle assessment of the
500 environmental performance of conventional and organic methods of open field pepper
501 cultivation system. The International Journal of Life Cycle Assessment, 1-13.
502 Chatzisymeon, E., Foteinis, S., Mantzavinos, D., Tsoutsos, T., 2013. Life cycle assessment of
503 advanced oxidation processes for olive mill wastewater treatment. Journal of Cleaner
504 Production 54, 229-234.
505 Foteinis, S., Kouloumpis, V., Tsoutsos, T., 2011. Life cycle analysis for bioethanol production
506 from sugar beet crops in Greece. Energy Policy 39, 4834-4841.
507 Frontistis, Z., Daskalaki, V.M., Hapeshi, E., Drosou, C., Fatta-Kassinos, D., Xekoukoulotakis,
508 N.P., Mantzavinos, D., 2012. Photocatalytic (UV-A/TiO2) degradation of 17α-ethynylestradiol
509 in environmental matrices: Experimental studies and artificial neural network modeling.
510 Journal of Photochemistry and Photobiology A: Chemistry 240, 33-41.
511 Frontistis, Z., Kouramanos, M., Moraitis, S., Chatzisymeon, E., Hapeshi, E., Fatta-Kassinos, D.,
512 Xekoukoulotakis, N.P., Mantzavinos, D., 2015. UV and simulated solar photodegradation of
513 17α-ethynylestradiol in secondary-treated wastewater by hydrogen peroxide or iron
514 addition. Catalysis Today 252, 84-92.
515 Frontistis, Z., Xekoukoulotakis, N.P., Hapeshi, E., Venieri, D., Fatta-Kassinos, D., Mantzavinos,
516 D., 2011. Fast degradation of estrogen hormones in environmental matrices by photo-
517 Fenton oxidation under simulated solar radiation. Chemical Engineering Journal 178, 175-
518 182.
519 Garrett , P., Collins, M., 2009. Life Cycle Assessment of Product Stewardship Options for
520 Mercury Containing Lamps in New Zealand: Final Report. Environmental Resources
521 Management (ERM), Ministry for the Environment, New Zealand.
522 Hermann, B.G., Kroeze, C., Jawjit, W., 2007. Assessing environmental performance by
523 combining life cycle assessment, multi-criteria analysis and environmental performance
524 indicators. Journal of Cleaner Production 15, 1787-1796.
525 Ioannou-Ttofa, L., Foteinis, S., Chatzisymeon, E., Michael-Kordatou, I., Fatta-Kassinos, D.,
526 2016. Life cycle assessment of solar-driven oxidation as a polishing step of secondary-treated
527 urban effluents. Journal of Chemical Technology & Biotechnology, n/a-n/a.
528 ISO, 2006a. ISO 14040:2006 - Environmental management -- Life cycle assessment --
529 Principles and framework. International Organization for Standardization, Geneva,
530 Switzerland (2006).
531 ISO, 2006b. ISO 14044:2006 - Environmental management -- Life cycle assessment --
532 Requirements and guidelines. International Organization for Standardization, Geneva,
533 Switzerland (2006).
534 Kouloumpis, V., Stamford, L., Azapagic, A., 2015. Decarbonising electricity supply: Is climate
535 change mitigation going to be carried out at the expense of other environmental impacts?
536 Sustainable Production and Consumption 1, 1-21.
537 Mohagheghian, A., Nabizadeh, R., Mesdghinia, A., Rastkari, N., Mahvi, A.H., Alimohammadi,
538 M., Yunesian, M., Ahmadkhaniha, R., Nazmara, S., 2014. Distribution of estrogenic steroids
539 in municipal wastewater treatment plants in Tehran, Iran. Journal of Environmental Health
540 Science and Engineering 12, 97-97.
541 OSRAM, 2016. Life cycle analysis of OSRAM products. OSRAM GmbH,, Hellabrunner Straße 1,
542 D-81543 München, Deutschland.

543 Rochester, J.R., 2013. Bisphenol A and human health: A review of the literature.
544 Reproductive Toxicology 42, 132-155.
545 Rodríguez, R., Espada, J.J., Pariente, M.I., Melero, J.A., Martínez, F., Molina, R., 2016.
546 Comparative life cycle assessment (LCA) study of heterogeneous and homogenous Fenton
547 processes for the treatment of pharmaceutical wastewater. Journal of Cleaner Production
548 124, 21-29.
549 Tiedeken, E.J., Tahar, A., McHugh, B., Rowan, N.J., 2017. Monitoring, sources, receptors, and
550 control measures for three European Union watch list substances of emerging concern in
551 receiving waters – A 20 year systematic review. Science of The Total Environment 574, 1140-
552 1163.
553 Zhang, Z., Ren, N., Kannan, K., Nan, J., Liu, L., Ma, W., Qi, H., Li, Y., 2014. Occurrence of
554 endocrine-disrupting phenols and estrogens in water and sediment of the Songhua river,
555 northeastern China. Archives of environmental contamination and toxicology 66, 361-369.

556

557

558

559 **List of Tables**

560 Table 1: Experimental data, taken from Frontistis et al. (2011, 2012, 2015), used to
561 build the LCI of light-driven AOPs.

562 Table 2: Electrical energy (E_{EO}) consumed by several light-driven oxidation
563 processes.

564 Table 1.

Light-driven process	Irradiation power, W	[TiO_2], mg/L	Power for water stirring, W	[Fe^{2+}], mg/L	H_2O_2, mg/L	Treatment time, min	EE2 removal, µg/L	Reference
Solar	150	-	30	-	-	60	2	(Frontistis et al., 2015)
Solar/Fe	150	-	30	5	-	60	46	(Frontistis et al., 2015)
	150	-	30	15	-	60	86	(Frontistis et al., 2015)
Solar/Fe/H_2O_2	150	-	30	5	10	15	98	(Frontistis et al., 2015)
	150	-	30	5	17.2	1	196	(Frontistis et al., 2011)
UVA	9	-	30	-	-	60	17	(Frontistis et al., 2015)
UVA/TiO_2	9	750	30	-	-	10	95	(Frontistis et al., 2012)
UVC	11	-	30	-	-	60	47	(Frontistis et al., 2015)
UVC/H_2O_2	11	-	30	-	10	15	100	(Frontistis et al., 2015)

565

566

567 Table 2.

Light-driven process	Irradiation power, kW	Volume, L	Treatment time to remove 90% of EE2, min	E_{EO}, kWh/m^3/order	Reference
Solar	0.150	0.3	2251	18758	(Frontistis et al., 2015)
Solar/Fe(5mg/L)	0.150	0.3	115	958	(Frontistis et al., 2015)
Solar/Fe(15mg/L)	0.150	0.3	70	583	(Frontistis et al., 2015)
Solar/Fe(5mg/L)/H_2O_2	0.150	0.3	2	17	(Frontistis et al., 2015)
UVA	0.009	0.3	312	156	(Frontistis et al., 2015)
UVA/TiO_2	0.009	0.3	7	4	(Frontistis et al., 2012)
UVC	0.011	0.3	113	69	(Frontistis et al., 2015)
UVC/H_2O_2	0.011	0.3	10	6	(Frontistis et al., 2015)

568

569

570 **List of Figures**

571 Figure 1. Environmental footprint of natural and simulated solar (a) photolysis and (b)
572 photocatalysis per functional unit, i.e. removal of 1 μg EE2 per liter of wastewater.

573 Figure 2. Environmental footprint of natural solar photocatalysis for removal of 1 μg
574 EE2 per liter of wastewater. Inset: environmental footprint of natural solar/Fe/H2O2
575 (17.2 mg/L).

576 Figure 3. Environmental footprint of UV-A and UV-C AOPs per functional unit
577 (removal of 1 μg EE2 per liter of wastewater).

578 Figure 4. Environmental footprint of natural solar, UV-A and UV-C photocatalysis
579 for removal of 1 μg EE2 per liter of wastewater.

580

581

582

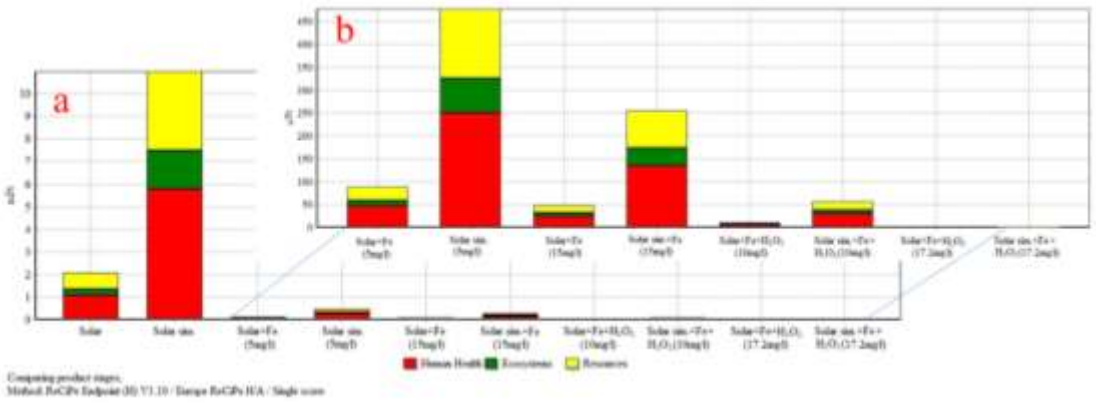

583

584 Figure 1.

585

586

587

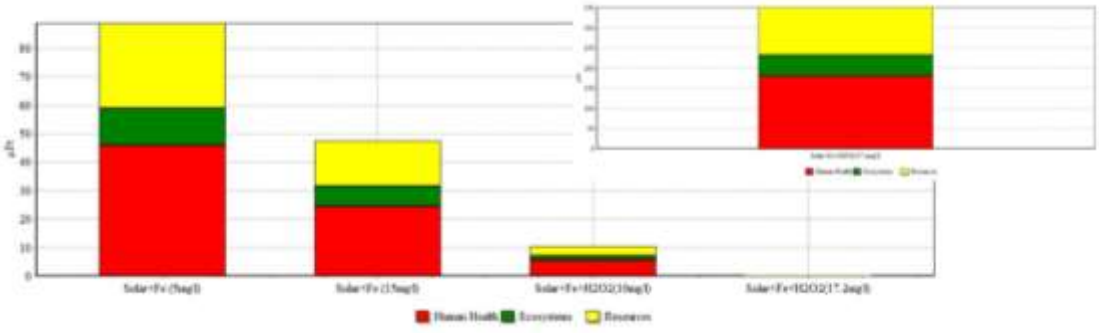

588

589 Figure 2.

590

591

592

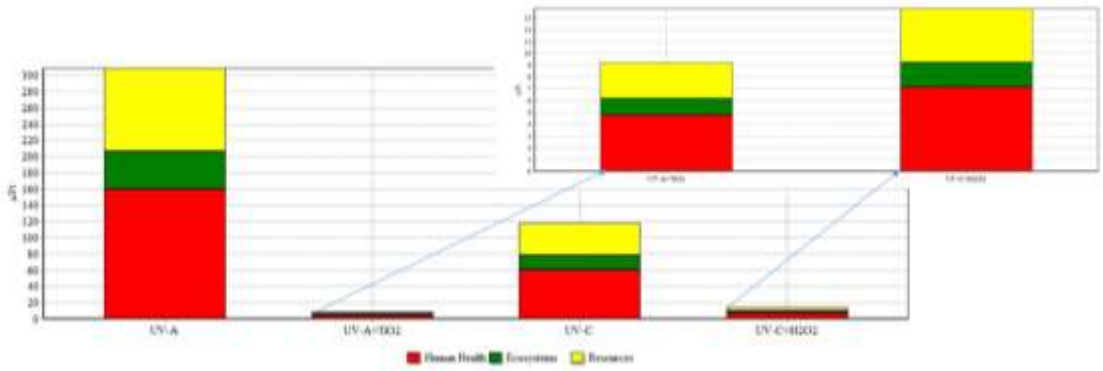

593

594 Figure 3.

595

596

597

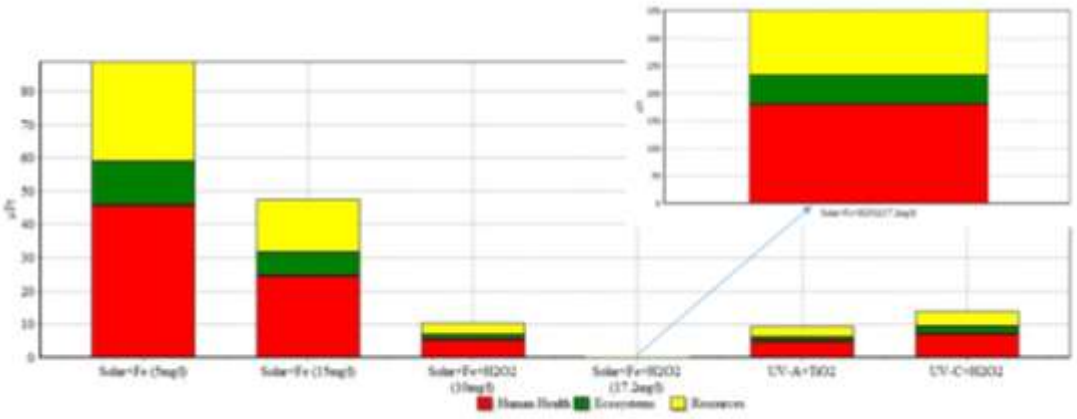

598

599 Figure 4.

600